Technologies for deposition of transition metal oxide thin films: application as functional layers in “Smart windows” and photocatalytic systems

2016 J. Phys.: Conf. Ser. 682 012011

(http://iopscience.iop.org/1742-6596/682/1/012011)

Technologies for deposition of transition metal oxide thin films: application as functional layers in "Smart windows" and photocatalytic systems

K Gesheva[1], T Ivanova[1], G Bodurov[1], I M Szilágyi[2,3], N Justh[2], O Kéri[2], S Boyadjiev[3], D Nagy[4] and M Aleksandrova[5]

[1] Central Laboratory of Solar Energy and New Energy Sources at the Bulgarian Academy of Sciences, "Tzarigradsko chaussee" 72 Blvd., 1784 Sofia, Bulgaria
[2]Budapest University of Technology and Economics, Department of Inorganic and Analytical Chemistry, Szent Gellért tér 4., Budapest, H-1111, Hungary;
[3]MTA-BME Technical Analytical Chemistry Research Group of the Hungarian Academy of Sciences, Szent Gellért tér 4., Budapest, H-1111, Hungary;
[4]University of Edinburgh, The King's Buildings, Mayfield Road, Edinburgh, EH9 3JL, UK
[5]Technical University Sofia, „St. Kliment Ohridski" 8 Blvd., 1756 Sofia, Bulgaria

E-mail: kgesheva@yahoo.com

Abstract. "Smart windows" are envisaged for future low-energy, high-efficient architectural buildings, as well as for the car industry. By switching from coloured to fully bleached state, these windows regulate the energy of solar flux entering the interior. Functional layers in these devices are the transition metals oxides. The materials (transitional metal oxides) used in smart windows can be also applied as photoelectrodes in water splitting photocells for hydrogen production or as photocatalytic materials for self-cleaning surfaces, waste water treatment and pollution removal. Solar energy utilization is recently in the main scope of numerous world research laboratories and energy organizations, working on protection against conventional fuel exhaustion. The paper presents results from research on transition metal oxide thin films, fabricated by different methods - atomic layer deposition, atmospheric pressure chemical vapour deposition, physical vapour deposition, and wet chemical methods, suitable for flow-through production process. The lower price of the chemical deposition processes is especially important when the method is related to large-scale glazing applications. Conclusions are derived about which processes are recently considered as most prospective, related to electrochromic materials and devices manufacturing.

1. Transition metal oxides

Transition metal oxides (TMO) are claimed to be one of the most interesting classes of solids, exhibiting varieties of properties, structures and applications [1]. Their properties are determined by the unique nature of their outer d-electrons. Transition-metal oxides can be insulators, semiconductors, metals, or undergo semiconductor-metal transitions. Transition metal oxides possess unusual and useful electronic, optical and magnetic properties. Many of these properties strongly depend on materials defects like vacancies, dislocations, stacking faults and grain boundaries [2].

TMOs are widely investigated due to their numerous applications. They are used as electrodes in electrochemical processes, functional components in technologically important catalytic processes. For example, they are used in selective oxidation, selective reduction and dehydrogenation. The catalytic properties of TMOs are defined of two main factors: these oxides exist in various crystallographic forms with closed stoichiometries with metal ions revealing different valence states and on the other hand, TMOs possess possibility for easy surface oxidation and reduction, which is related to high densities of cations and anions vacancies.

Other interesting application includes gas sensors [3-9], where a gas sensitive oxide (such as WO_3 or MoO_3) responses to the presence of certain gas by changing e.g. their electrical properties (resistance). The layered structured TMO (MoO_3,V_2O_5, MnO_2) can play role in lithium micro batteries, based on reverse injection of Li^+ ions in the host crystal lattice. The transition metal oxides can be used in high density memories, optical devices, passive display electrodes, magnetic recording and holographic devices, fuel cells, micro electronic circuits.

In this paper, the electrochromic and photocatalytic properties of TMO will be briefly reviewed.

2. Electrochromic devices

The chromogenic phenomenon is a reverse optical change under external influences. Electrochromism is a physical phenomenon describing reversible optical absorbance change of electrochemically active materials upon an application of electrical potential [10]. Recently, the electrochromic materials gain a lot of attention due to the energy saving applications and usage as smart windows [11], anti-glared rear view mirrors [12], and displays [13].

Electrochromic material (often in thin film form) is a part of electrochromic device [14], which is typically consisted of several components (see figure 1): a glass substrate covered by transparent conducting oxide (TCO); an EC film (transition metal oxides and mostly WO_3); an ion conductor (IC) (a polymer electrolyte or solid one); a counter electrode – often this is also conductive glass substrate with anodic type electrochromic functional film.

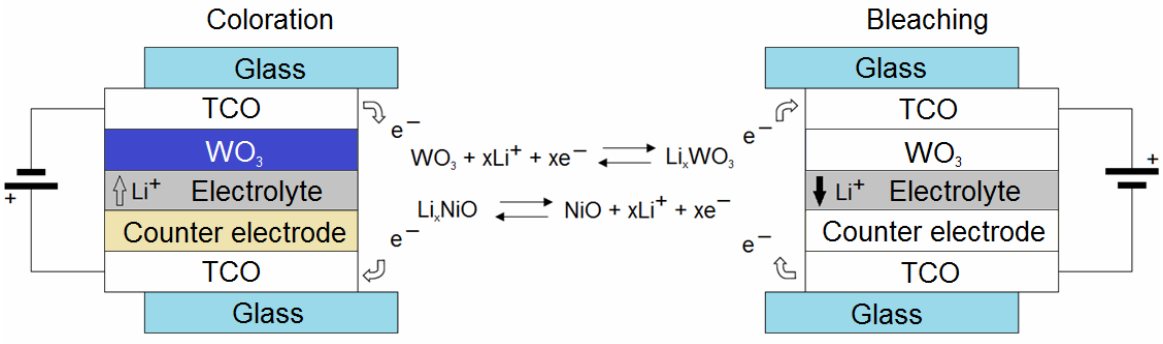

Figure 1. Schematically representation of an EC multilayer stack

The configuration of an EC device has sometimes compared to battery [14]. There are three types of electrochromic device (EC) designs: battery-like type, solution phase type and hybrid type, shown on figure 2. In the solution type design, both of the redox systems are dissolved in liquid solutions. And finally, in hybrid type design, one of the redox systems is in the form of a solid film, while the other is dissolved in a liquid solution. It is important to note here, that the solution and hybrid types are self-erasing, while the battery type EC devices have memory effect (the ability to retain colour even in open circuit, which implies high energy savings).

Cathodic type electrochromism is referred to materials that become absorptive when the alkali ions are injected or anodic electrochromism – optical absorption is decreased under ions intercalation. These cathodic and anodic oxides can be combined in devices to form smart windows resulting in a rather neutral visual appearance [15] and thus making them very suitable for general applications in

architecture. The most commonly used oxides are based on Wand Ni and exhibit cathodic and anodic electrochromism. Among the other Transition Metal Oxides (TMO) used in electrochromic applications, tungsten trioxide (WO_3) [16, 17] is the most studied one due to its promising electrochromic properties such as high coloration efficiency and short switching time. Commercial electrochromic devices require improvement in the EC properties since the bright blue color of WO_3 films in the reduced state is not favorable as bronze or pale yellow colors for most building applications. It has been proved that better electrochromic performance can be achieved by the addition of dopants to WO_3 [18]. It is also reported that color neutrality can be obtained by vanadium doping in tungsten oxide. Optical absorption in these vanadium doped films is due to polaronic transition V^{4+}, V^{5+} and W^{5+}, W^{6+} in WO_3 [19]. The interaction between WO_3 and V_2O_5 is unique because of the similarities of ionic radii and the structure in their highest oxidation state [20].

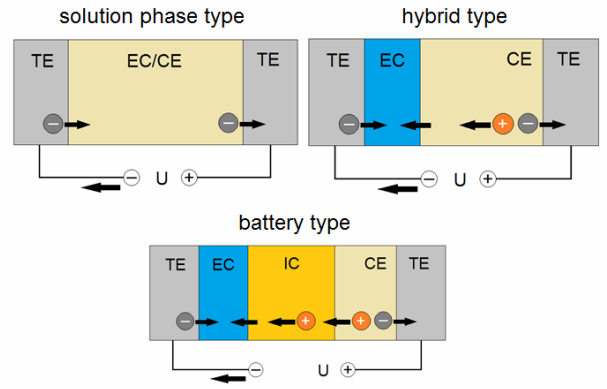

Figure 2. Different types of EC devices, where TE is transparent conducting electrode, EC - electrochromic electrode, CE – counter electrode and IC is ion conductor, respectively. The smart windows are considered from the battery type.

Another very interesting material is molybdenum oxide, which is found to be cathodic type electrochromic film with possibility for revealing great color densities. MoO_3 as a wide band gap semiconductor is a transparent in the visible spectral range and with crystal structure that allows easy intercalation/deintercalation of small ions. Molybdenum exists in different crystalline oxide modifications and can easily produced substochiometric structures. The two basic crystal phases are a unique layered structure (α - MoO_3 with orthorhombic symmetry) and metastable monoclinic β - MoO_3 (see figure 3). These phases differ in their vibrational and optical properties.

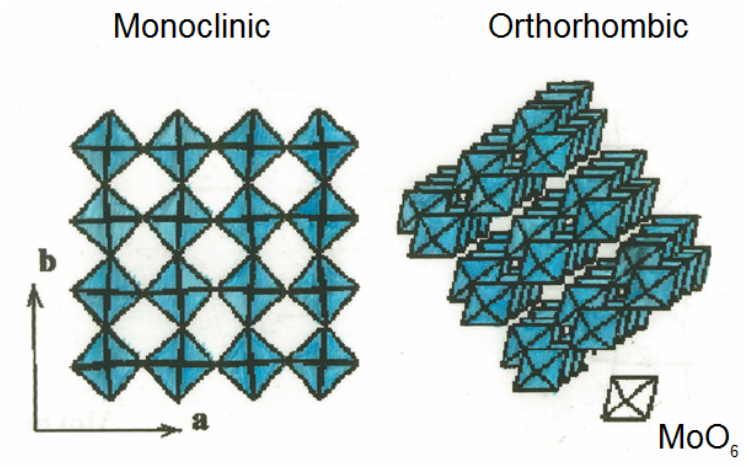

Figure 3. Schematic presentation of a) monoclinic β and b) orthorhombic α - phase of MoO_3

They exhibit different refractive indices and optical band gap energy values [21]. The orthorhombic MoO_3 possess unique two-dimensional space layered structure, consisting of distorted MoO_6 octahedra with common edges and corners. Each octahedron possess one connected oxygen atom, two O atoms are common for two octahedra and three O atoms are with common corners and are shared for three octahedra, approaching the complete stoichiometry - $MoO_1(O_{1/2})_2(O_{1/3})_3$. The double layers are characterized with sublayers from periodically arranged MoO_6, where the oxygen atoms participate inside the adjacent octahedra into and among the sublayers. The internal interaction among atoms is dominated by ionic and covalent forces, but the sublayers pair is interacted by weak van der Vaals forces [22]. This structure gives opportunity for injection of different donor ions into interlayered spaces and favors EC properties. In contrast, the metastable monoclinic β - phase has a cubic ReO_3 - like structure, consisting of three-dimensional rows from shared MoO_6 octahedra [23]. Spontaneous transformation $\beta \rightarrow \alpha$ phase occurs at temperatures of 370-400^{o}C.

The main characteristic of MoO_3 films can be summarized as follows [24, 25]: excellent electrochemical stability; low cost; cyclic stability; a stronger and more uniform absorption of light in its colored state (molybdenum bronze); a better open-circuit memory than a majority of TMOs; molybdenum bronze is more akin to the sensitivity in human visual perception.

Binary combinations of oxides have been investigated to improve or modify the optical and electrical properties of different oxides and even to tailor their properties in predictable way. Possible beneficiary effects for mixing two electrochromic materials are to obtain increased coloration efficiency, improved durability, color neutrality, a larger switching potential range or faster reaction kinetics [26]. Mixed MoO_3-WO_3 films can show higher electrochromic efficiencies as a result of enhanced electron intervalence transfer between Mo^{5+} and W^{6+} states, and W^{5+} to W^{6+} transitions [27]. Optically, it is expected that the absorption peak of the tungsten/molybdenum mixed oxide films is shifted notably toward the eye-sensitive peak, and therefore electrochromic performance of the films is significantly increased [28].

Our group has been investigated MoO_3, WO_3, mixed Mo-W and W-V oxides films with respect to their optical and electrochromic behaviour [29]. The chosen technological approach for deposition of electrochromic functional films is APCVD (atmospheric pressure chemical vapour deposition).

3. Atmospheric pressure chemical vapour deposition - technology

CVD technology can be applied for obtaining a wide spectrum of thin film materials such as metals, semiconductor III-V compounds, dielectric oxides, perovskite heterostructures, magnetics and conductors. It is especially useful for fabrication of nanosized layers, nanoparticle and nanotubes (graphene and carbon nanotubes), free standing diamond films, etc. Recently, it has been found that although CVD is traditionally not compatible with polymer thin-film deposition, through modifications of the CVD reactants or reactor designs, polymer depositions at low temperatures and low-energy inputs can be achieved, making CVD a widely used technique for polymer deposition [30, 31]

CVD possesses some advantages over physical deposition methods and other chemical technologies such as:

- Broad group of high purity depositing thin films
- Possibility for covering flat and complex substrate morphologies
- Selective growth on chosen part of the substrates
- Different properties by varying deposition parameters
- Film deposition at low temperatures
- Preparation of single layer, multilayered structures, composites and functional coatings
- APCVD is compatible with industrial manufacturing, and for electrochromic application it can be integrated in in-line glass production [32].
- In order to achieve greater deposition rates and to lower deposition temperatures CVD processes can be enhanced by plasmas, ions, lasers, photons etc means, which can even further to broaden the materials that can be deposited by this technology.

On the other hand, this method also shows some disadvantages:

- Complexity of chemical reactions into CVD reactors
- Possible contaminations from precursors to the film structures
- Limitation of substrate choice due to possible diffusions or alloying
- Careful choice of precursors as they must be volatile at low temperatures, chemically stable, not toxic or poisonous, well designed for surface reaction to appear.
- Some by-products of CVD reactions can be hazardous (CO_2, HF or H_2)

In real technological CVD reactors, it is common to have heterogeneous and complex reactions near to heated substrates. In order to predict and obtain information for deposition under specific conditions, a thermodynamic modulation is usually performed, including data for free energy of formation of every gaseous and solid components. But as it is mentioned for a CVD process, there is a multi component and multi phase system, which makes its theoretical description very difficult [33]. Modelling can then be used to predict growth rate, etching rate, surface morphology and doping, all key aspects when doing CVD of electronic device structures.

The APCVD equipment used in the present research for deposition of MoO_3, WO_3, Cr_2O_3, mixed Mo-W and W-V oxides films consists of horizontal quartz reactor with cold walls. A graphite susceptor covered with SiC coating is used as substrate holder and the heating is realized with the help of high frequency (HF) generator. The used precursor is placed in special sublimator, immersed into silicon oil bath, heated by magnetic stirrer at certain temperatures. The precursor vapors are carried from the sublimator to the CVD reactor by an argon flow through heated Teflon tubes. From a separate gas line, O_2 enters into the reactor. In the CVD reactor around the hot substrates gas reaction condition is created at a local thermodynamic equilibrium, which leads to oxide deposits.

This configuration of CVD reveals some advantages:

- The cold wall reactor allows to obtain deposits only on the heated substrates, and the control of substrate temperature is easier
- The atmospheric pressure allows more homogenous reactions and appearence of quasi thermodynamical equilibrium in areas near the substrates
- Varying technological parameters (substrate and sublimator temperatures, gas flow rates (Ar and O_2), deposition time) can lead to films with different properties

4. APCVD MoO_3-WO_3 films – electrochromic characteristics

Metal oxide films of MoO_3, WO_3, and mixed MoO_3-WO_3 films were deposited by carbonyl CVD process at atmospheric pressure. The powder source consisted of the two carbonyl precursors in a certain ratio ($Mo(CO)_6$:$W(CO)_6$=1:4) and this mixture was heated in silicon bath at the temperature of 90^{o}C. For the comparative study the deposition temperature was kept at 200^{o}C because only at this temperature it was possible for the three kinds of metal oxide films to be deposited. Visually, the as-deposited films are slightly coloured: bluish (WO_3), yellowish (MoO_3) and brownish (MoO_3-WO_3). The deposition time was kept constant (40 min) and because of the different growth rates the film thickness was 300 nm for MoO_3, 400 nm for WO_3 and 120 nm for MoO_3-WO_3. As a result, mixed films were successfully deposited and they were visually transparent and uniform [34].

The mixed oxide films are expected to improve the electrochromic behavior. The doping of MoO_3 in WO_3 structure leads to different electrochromic effect. Deposition of CVD MoO_3-WO_3 films from mixed precursor $Mo(CO)_6$:$WO(CO)_6$= 1:1 were previously performed keeping the optimal gas flow ratio 1/32 [35]. For these samples, the optical modulation varies in the range of 30-50% and the estimated color efficiency values were 25-30 cm^2/C in electrolyte 1M $LiClO_4$ + PC (propylene carbonate). These values are much smaller than those of MoO_3-WO_3 films deposited from precursor mixture 1:4, in which $Mo(CO)_6$ prevails, showing colour efficiency CE = 114 cm^2/C and optical modulation around 70% at a wavelength λ = 550 nm [36]. Investigations were carried out on these Mo-W oxide films in Li^+ containing electrolyte at different scan rates. The results show that increasing scan rate (corresponding to faster intercalation/deintercalation rates) results in smaller values of the electrochromic characteristics. It was determined that the colour efficiency values vary in the range 40

– 77 cm^2/C and 18 – 30 % optical modulation at a scan rate 50 mV/s. The highest electrochromic color efficiency is obtained at scan rate (10 mV/s) at wavelength 550 nm - the maximum of the human eye sensitivity. The effect can be proposed to originate from the molybdenum oxide presence into the films.

Electrochemical studies were also performed to reveal the behavior of CVD MoO_3-WO_3 films under different ion insertion mechanisms. The measurements were carried out to observe the influence of two type proton electrolytes - 1 M H_2SO_4 and 1 M H_3PO_4, comparing with 1 mol/l $LiClO_4$+PC electrolyte. It must be pointed out that MoO_3 films are found to be stable in acidic electrolytes and WO_3 films are destroyed, but mixed oxide films show no change of its electrochromic properties after long term cycling and therefore, they are also successful studied in proton type liquid electrolytes. The estimated electrochromic characteristics are shown at figure 4. The smallest values are found for phosphorous acid electrolyte. The obtained electrochromic parameters manifest strong wavelength dependence. When the used electrolyte was 1 M H_2SO_4+glycerine the highest values are 84 cm^2/C (λ=750 nm), 100.5 cm^2/C (λ=700 nm) and 120 cm^2/C (λ=650nm) and there they exceeded even those of Li electrolyte. In the same time in the spectral range 500-600 nm the best results are observed for1 mol/l $LiClO_4$+PC [37].

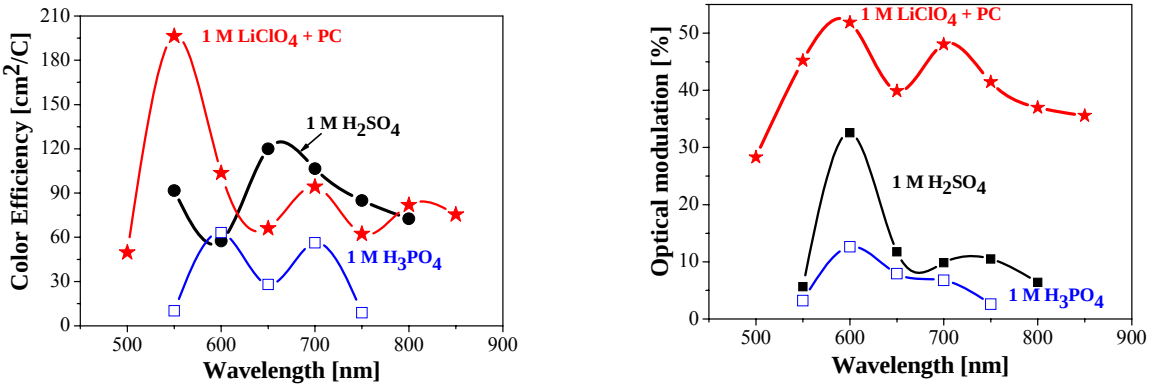

Figure 4. Electrochromic characteristics of CVD MoO_3-WO_3 films, derived from cyclic voltametric measurements in three types of electrolytes [37].

5. Flexible transparent conductive substrates

In the recent years the optoelectronic devices produced on flexible substrates have become very popular due to their light weight, thinness and portability in comparison to the glass based devices. The most studied applications (electrochromic displays, electroluminescent light-emitting diodes, solar cells) contain multilayer stack of different materials deposited on plastic substrate of polyethylene terephthalate (PET) [38-40]. One of the most spread, commercially developed transparent electrode for the glass based version of these devices is indium-tin-oxide (ITO). It has been found that ITO is brittle for the flexible analogues and cracks are revealed at low tensile strain, multiple bending or folding [41]. In contrast to ITO, the conductive polymer poly(3,4-ethylenedioxythiophene) polystyrene sulfonate (PEDOT:PSS) is an perspective alternative for transparent electrode in the flexible optoelectronic devices due to its superior mechanical properties, such as high elasticity, coefficient of thermal expansion closer to that of the plastic substrates, as well as cheaper and easier processing [42]. The low free surface energy of the flexible substrates such as PET, polyethylene sulfonate (PES) or polyethylene naphtalate (PEN), leads to poor adhesion of the PEDOT:PSS coatings and therefore additional surface modification is required, such as plasma or solvent treatment [43]. Such methods, however, change the chemical composition of the polymer surface, increase the surface roughness, or may induce thermal stress in the plastic substrate. To avoid these drawbacks Aleksandrova et. al. suggested UV treatment of PET, before deposition of PEDOT:PSS [44].

For PET surface modification, a mercury lamp with a power of 200 W and a wavelength of 365 nm was used. For comparison of the properties of UV/PET-PEDOT: PSS electrodes with those of the conventional ones, ITO films with same thickness of 35 nm were RF sputtered on PET. To demonstrate the electrode efficiency of UV treated PET/PEDOT:PSS, a simple single layer organic light emitting device (OLED) was prepared by spin coating of a 150 nm electroluminescent film of poly[2-methoxy-5-(2-ethylhexyloxy)-1,4-phenylenevinylene] (MEH-PPV) on the PEDOT:PSS (spin coated as well). Aluminum top contacts were thermally evaporated in vacuum via shadow mask.

The mechanical stability in term of bendability of the UV treated and non-treated PET with deposited PEDOT:PSS films were estimated by lab-made electromechanical setup for tension test (figure 5). The strain applied to the substrate is related to the force intensity generated by the electromechanical system. The force is alternative and its frequency can be tuned. For these experiments a force with an intensity of 25 N from peak to peak and constant frequency of 50 Hz was supplied to the sample. The total number of bends was obtained by setting different time durations of the applied cyclic force. A four point probe FPP5000 resistance measurement system was used to measure the change in the sheet resistance of the films after different numbers of mechanical loads. Optical microscopy at x500 magnification was used to observe cracks revealed in the films after bending.

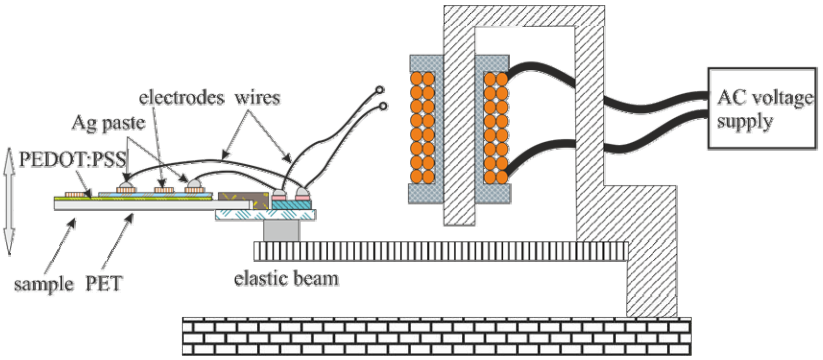

Figure 5. Experimental setup for dynamic mechanical loading applied on the flexible substrates coated by transparent conductive films [43].

XPS measurements showed that UV exposure influences the carboxyl bonds strength from the PET surface and modifies the oxygen functional groups [45]. It was proved that UV treatment causes incorporation of oxygen groups on the PET surface, which results in increasing free energy and improves the surface wettability. Higher wettability resulted in better distribution of the polymeric film. XPS analysis also confirmed that the exited non-bonded oxygen atoms on the PET surface possess energy close to the energy of the oxygen atoms in the bonds with sulfur atoms in the PSS chain, which exceeds the energies of the PSS– H^+ and C–O–C bonds in the PEDOT backbone [46]. This is an indication for their oxidation from the oxygen atoms of the PET surface and bonding with the surface functional groups. This is in agreement with a greater adhesive strength at the PEDOT: PSS/PET interface, and a more favorable behavior in multi-bendable devices is expected for the PEDOT:PSS deposited on the UV treated PET. It was found that PEDOT:PSS film adhesion to the PET substrate is stronger on the UV treated substrate surface. At 50 N/cm^2 tensile force and a peel angle of 90^o the coating still remained on the PET surface. For the untreated substrates the films peeled off from the surface at typically 19 N/cm^2, probably due to lack of uniformity of the distributed solution at spin coating on hydrophobic surface. It results in formation of irregularities in the PEDOT:PSS film, that can cause strain forces and can be reason for poor adhesion.

Figure 6 shows the change of the film's sheet resistance under repeated bends and allows estimation of the films stability. According to the bending tests, the PEDOT:PSS film deposited on UV treated PET exhibits only 3.8% resistance change in the entire range of bending cycles. The initial

resistance of the samples was close to that of conventional ITO (52.4 Ω/sq and 50.5 Ω/sq for ITO) and stays stable after repeating mechanical loading. This can be explained by the higher adhesion strength at the PET interface. The weaker adhesion of PEDOT:PSS deposited on untreated PET leads to a less stable electrical behavior as a greater resistance change of 8.7% is observed. The initial resistance of 57 Ω/sq was the highest measured. The ITO transparent coating shows the greatest change in its resistance of 23.5 %.

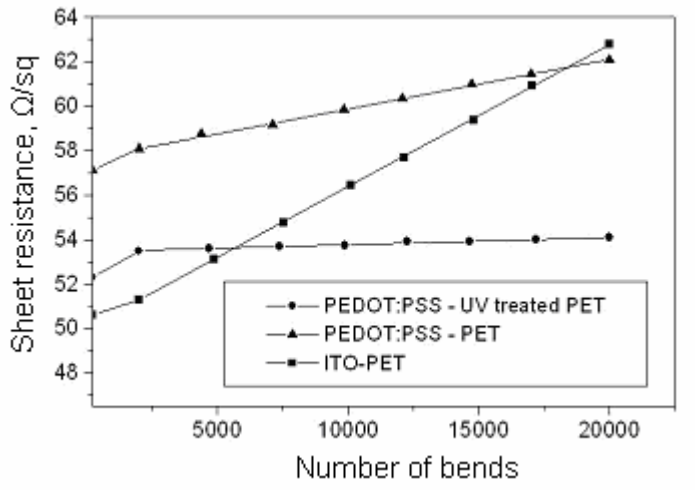

Figure 6. Sheet resistance change at different numbers of bends for PEDOT:PSS deposited on UV treated and untreated PET. ITO on PET was used as a reference [44].

Figure 7 presents microscopic images of the PEDOT:PSS films deposited on UV treated and untreated PET, as well as of ITO deposited on PET. As can be seen when 5000 cycles of mechanical loading was applied to the samples no significant effect was observed in the UV treated PEDOT:PSS film's morphology (figure 7 a). This is in agreement with the results obtained for the stable sheet resistance and the higher adhesive strength. Bending cycles induced cracks in the ITO coating that propagated laterally to the loading direction, leading to fast physical degradation and instability in the sheet resistance (figure 7 b).

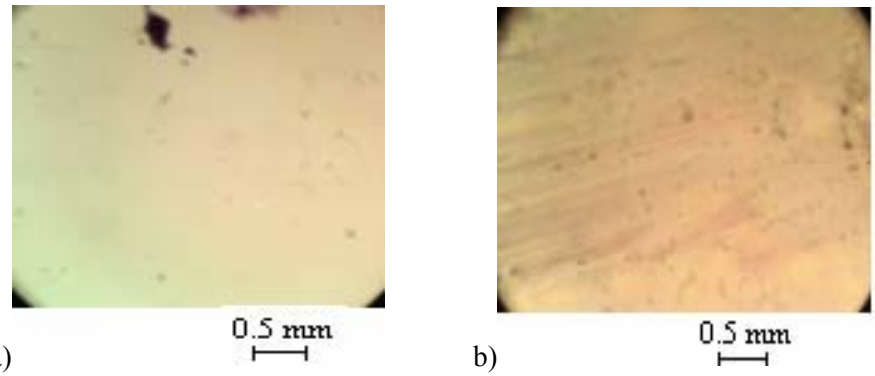

a) b)

Figure 7. Microscopic images of films' surfaces after 5000 bends a) PEDOT:PSS on UV treated PET; b) ITO on PET [43].

Figure 8 represents the current-voltage characteristics of single layer flexible OLED device with PEDOT:PSS electrode on UV treated and non-treated PET, as well as with conventional ITO.

Both curves are similar to that of diode structure, but for the PEDOT:PSS based device the turn on voltage is higher and the current at given constant voltage is smaller due to the higher sheet resistance in comparison to ITO.

Optimization of the emissive recombination is out of the aim in this work, as the main indication for working sample is the current, flowing through the interfaces. Nevertheless, this characteristic

proves the successful fabrication of flexible OLED with material alternative to ITO for transparent conductive electrode, which is more stable at repeating bends.

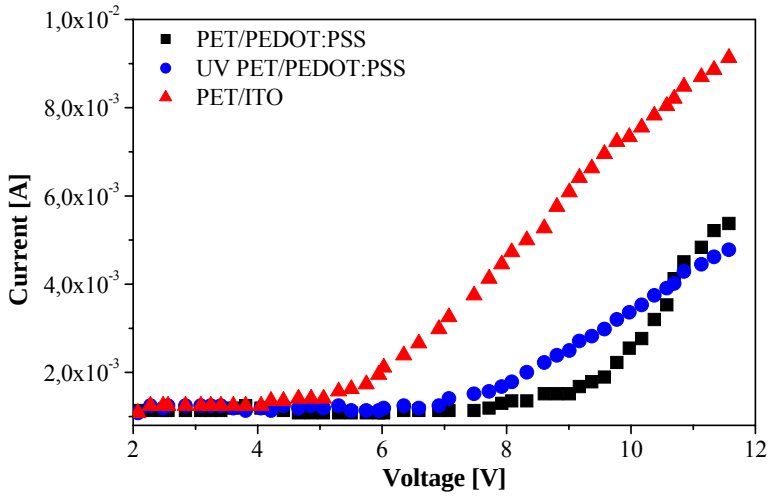

Figure 8. Current -voltage characteristics of the flexible OLED with PEDOT:PSS anodes on UV treated and non-treated PET substrate. Device with ITO anode was used as control sample [45].

6. Photocatalysis

Civil, commercial and industrial sectors are all facing environmental problems related to hazardous wastes, toxic air and contaminated waters. The elimination of toxic and hazardous chemicals has become an international priority. Due to this interest in application of photocatalysis for these environmental problems has grown exponentially, which enables waste water treatment, pollutant decomposition and self-cleaning of surfaces by the use of sunlight.

Transitional metal oxides are the most prominent photocatalytic materials. When the energy of an absorbed photon matches or exceeds the bandgap energy of the TMOs, an electron (e^-) is promoted from the valence band into the conduction band, leaving a hole behind (h^+). On the one hand, these electrons and holes can participate in redox reactions of decomposing pollutants, or they can react with water, which leads to the production of reactive ·OH or $\cdot O_2^-$ species, which can also react with hazardous molecules. On the other hand, the electrons and holes can recombine easily, which might result in lowering the photocatalytic efficiency.

TMO materials in photocatalysis were already used for the remediation of a wide variety of contaminants (e.g. alkanes, alkenes, phenols, etc.). In many cases, complete mineralization of the contaminant has been reported. The most common photocatalysts are WO_3, ZnO, TiO_2, SnO_2. TiO_2 is the most widely-spread TMO photocatalyst because it has the best conduction band and bandgap energy levels for water splitting. The only disadvantage of TiO_2 is that its absorption range is in UV, while e.g. WO_3 absorbs also visible light. To increase the efficiency of photocatalysis (and especially of TiO_2), an option is doping with heteroatoms (C, N, S), dye molecules or other organic compounds, as well as with a visible light active TMO, which widen the absorptions range more to the visible spectrum as well. Another way to reach better photocatalytic activity is decreasing the recombination rate of photogenerated electrons and holes by making composites of the TMO with noble metals (e.g. Au, Ag), carbon nanostructures, or with other TMO materials [47-51].

7. Atomic layer depositon (ALD)

Besides CVD another way to deposit TMO thin layers, which can be used as photocatalysts or electrochromic materials is atomic layer deposition. The beginning of the theory of ALD dates back to the 1950s to St. Petersburg, where then Aleskovskii and Koltsov made the first experiments in the 1960s with the method they called molecular layering (ML). Independent of them in Helsinki, Suntola

and coworkers also developed a method named atomic layer epitaxy (ALE), and it was them in the 1970s, who enabled ALE to be used widely in the industry. As the dimensions decreased in the semiconductor industry, it led to the demand for atomic level control of conformal, thin film deposition (especially of the high-κ oxides); thus, now the method called ALD started to gain increased international interest in the 1990s. Then in the 2000s ALD also reached nanotechnology, and was used to fabricate sensors, solar cells, catalysts, nanocoatings, nanocomposites, etc.

ALD is able to meet the needs for atomic layer control and conformal deposition using sequential, self-limiting surface reactions. A general ALD reaction has four consecutive steps: (1) the first precursor is pulsed into the reactor, which chemisorbs on the surface of the substrate; (2) the unreacted precursor and reaction by-products are removed by an inert gas purge and/or by evacuation; (3) the second precursor is pulsed, which reacts with the first precursor solely on the surface; (4) the unused second precursor and the reaction by-products are removed.

The advantages of ALD are precise thickness control at monolayer level and self-limiting growth. The film thickness can be planned easily by the number of the ALD cycles and the self-limiting aspect of ALD leads to excellent step coverage and conformal deposition. The composition of the film can also be controlled precisely. ALD can use solid, liquid or gaseous precursors (elements, molecules or radicals), and the main requirement is that they have to be volatile. ALD can be used to deposit elements (Au, Ag, Pt, Ru, Fe, etc.), binary compounds (e.g. oxides, nitrides, carbides, sulfides, fluorides, like Al_2O_3, TiO_2, ZnO, HfO_2, GaN, TaC, CaS, SrF_2, etc.), ternary compounds (e.g. $MgAl_2O_4$, TiAlN), polymers, organic and hybrid materials. The usual reaction temperature is between 100-400°C, and the ideal reaction temperature zone is often described by the so-called ALD window. Usually ALD reactions take place in vacuum, but it is also possible to grow thin films by atmospheric pressure ALD or at lower temperatures.

ALD and CVD have many similarities, yet there are several distinctive features. In ALD the precursors enter the reactor separately, thereby eliminating gas-phase reactions. ALD film growth frequently occurs at lower temperatures compared to CVD processes because of the elimination of the gas-phase reactions. In ALD there is no shadow effect, which might reduce the growth rate if there is an object between the source and the target [52-56].

There are only few ALD reactions yet, which can be used to deposit WO_3 and MoO_3. There are two molybdenum precursors reported for MoO_3: $C_{12}H_{30}N_4Mo$ [57] and $Mo(CO)_6$ [58]. Likewise there were two kind of tungsten precursors used for WO_3: $W(CO)_6$ [59-61] and $W_2(NMe_2)_6$ [62]. The oxygen precursors were H_2O for thermal ALD and ozone (O_3) for plasma ALD processes, both in the case of WO_3 and MoO_3. The MoO_3 has a tight ALD window with the range of 152-172 °C, while there were successful depositions of WO_3 films from 150-300 °C.

8. Photocatalytic thin films and nanostructures prepared by ALD

For photocatalytic water-splitting MoO_3–WO_3 composite films were successfully prepared by APCVD [63]. In contrast, in the few studies which described the deposition of MoO_3 and WO_3 by ALD, the photocatalytic properties were not studied, and there are also no studies yet of using ALD materials as elelctrochromic layers. Nevertheless, there are a large number of papers, which report about the photocatalytic use of ALD deposited materials. Regarding the photocatalytic thin films and nanostructures prepared by ALD, it was TiO_2 as TMO material, which was mostly grown by ALD.

On the one hand, photocatalytic TiO_2 thin films were grown by ALD on various planar substrates. The composition of such thin films can be finely tuned by ALD, which was demonstrated by e.g. doping with S by adding a third (H_2S) precursor besides $TiCl_4$ and H_2O, or with F atoms by exchanging the $TiCl_4$ precursor with TiF_4. Due to the doping, the absorption of TiO_2 was shifted to the visible range, and this resulted in photocatalytic activity also under visible light illumination [64-65].

On the other hand, and this is the more frequent case, various nanostructured substrates (e.g. nanoparticles, nanotubes, nanowires, nanopatterned surfaces, etc.) were also covered with photocatalytic TMO layers by ALD. Although photocatalytic WO_3 and MoO_3 layers were not deposited yet by ALD, WO_3 nanowires prepared by electrospinning [66] were used as substrates for

ALD TiO_2 thin films. The as-obtained WO_3/TiO_2 core/shell nanofibers (figure 9) were both UV and visible light active photocatalysts [67]. By combining electrospinning and ALD it is also possible to prepare photocatalytic magnetic particle loaded nanotubes [68], while by using electrospinning, ALD and hydrothermal synthesis photocatalytic hybrid ZnO nanoneedle decorated polymer fibres can be produced [69]. Photocathodes to produce hydrogen through water photoelectrolysis can be prepared by covering silicon nanobelts arrays by thin TiO_2 protection layer using ALD [70]. A very interesting example of self-cleaning photocatalytic surfaces was obtained, when TiO_2 layers were grown on lotus leaves to yield a superhydrophobic and photocatalytic bionanocomposite with tuneable properties [71].

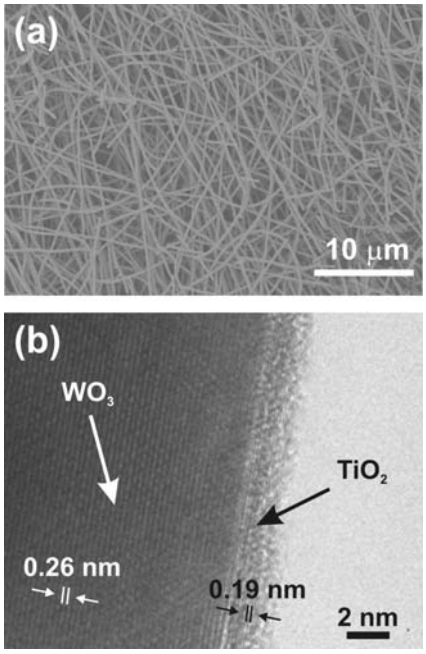

Figure 9. (a) SEM image of electrospun WO_3 nanofibers; (b) HRTEM image of the photocatalytic WO_3/1.5 nm TiO_2 core/shell nanofibers composite [67]. (Copyright Wiley-VCH Verlag GmbH & Co. KGaA. Reproduced with permission.)

9. Conclusions

In this paper the application transitional metal oxides were presented both in electrochromic devices and photocatalytic reactions. The thin films of TMOs were grown by CVD, APCVD or ALD. For comparison results of Physical Vapor Deposition are also given. The theory of these thin films deposition methods was discussed, and numerous examples were presented in which MoO_3, WO_3 and TiO_2 layers were grown for electrochromic and photocatalytic applications.

Acknowledgements

This paper was presented at INERA Conference Workshop "Light in Nanoscience and Nanotechnology 2015", October 20-22th, 2015, Hissar, Bulgaria. The Conference is part of the Program of INERA REGPOT Project of Institute of Solid State Physics, Bulgarian Academy of Sciences.

I. M. S. thanks for a János Bolyai Research Fellowship of the Hungarian Academy of Sciences and an OTKA-PD-109129 grant. S. Boyadjiev thanks the Postdoctoral Fellowship programme of the Hungarian Academy of Sciences (2013-2015).

References

[1] Rao C N R 1989 *Ann Rev Phys Chem* **40** 291
[2] Kung H H 1989 *Transition Metal Oxides: Surface Chemistry and Catalysis*, Elsevier Science, NY
[3] Li X L, Lou T J, Sun X M and Li Y D 2004 *Inorg Chem* **43** 5442

[4] Boyadjiev S, Georgieva V, Vergov L, Baji Z, Gáber F and Szilágyi I M 2014 *J Phys Conf Ser* **559** 012013
[5] Szilágyi I M, Saukko S, Mizsei J, Tóth A L, Madarász J and Pokol G 2010 *Solid State Sci* **12** 1857
[6] Szilágyi I M, Wang L, Gouma P I, Balázsi C, Madarász J and Pokol G 2009 *Mater Res Bull* **44** 505
[7] Szilágyi I M, Madarász J, Pokol G, Király P, Tárkányi G, Saukko S, Mizsei J, Tóth A L, Szabó A and Varga-Josepovits K 2008 *Chem Mater* **20** 4116
[8] Szilágyi I M, Saukko S, Mizsei J, Király P, Tárkányi G, Tóth A L, Szabó A, Varga-Josepovits K, Madarász J and Pokol G 2008 *Mater Sci Forum* **589** 161
[9] Balázsi C, Wang L, Zayim E O, Szilágyi I M, Sedlackova K, Pfeifer J, Tóth A L and Gouma P I 2008 *J Eur Ceram Soc* **28** 913
[10] Kao S Y, Lin Y, Hu C W, Leung M and Ho K 2015 *Solar Energ Mater Solar Cell* **143** 174
[11] Sabry M, Eames P C, Singh H and Wu Y 2014 *Solar Energ* **103** 200
[12] Granqvist C G 1995 *Handbook of Inorganic Electrochromic Materials*, Elsevier Science, Amsterdam
[13] Cheng C P, Kuo Y, Cheng C H and Zheng Zh W 2014 *Solid State Electr* **99** 16
[14] Heckner K H and Kraft A 2002 *Solid State Ionics* **152-153** 899
[15] Granqvist C G 2014 *Thin Solid Films* **564** 1
[16] Tuna O, Sezgin A, Budakoglu R, Turkuz S and Parlar H 2015 *Vacuum* **120** 28
[17] Gogova D, Stoyanov G and Gesheva K 1996 *Renewable Energy* 8 546
[18] Meenakshi M, Gowthami V, Perumal P, Sivakumar R and Sanjeeviraja C 2015 *Electrochim Acta* **174** 302
[19] Li Z, Liu H, Liu Y, Yang S and Yan Liu Y 2010 *Proc SPIE* **7654** 765411
[20] Najbar M, Camra J, Białas A, Wesełucha-Birczyńska A, Borzecka-Prokop B, Delevoye L and Klinowski J 1999 *Phys Chem Chem Phys* **1** 4645
[21] Livage J and Ganguli D 2001 *Solar Energ Mater Solar Cell* **68** 365
[22] Stjerna B, Olsson E and Granqvist C G 1994 *J Appl Phys* **76** 3797
[23] Kuwabara K, Sugiyama K and Ohno M 1991 *Solid State Ionics* **44** 313
[24] Shen Y, Yang Y, Hu F, Xiao Y, Yan P and Li Zh 2015 *Mater Sci Semicond Proc* **29** 250
[25] Lin T N, Lin Y H, Lee C T, Han S and Weng K W 2015 *Thin Solid Films* **584** 341
[26] Patil C E, Tarwal N, Jadha P, Shinde P, Deshmukh H, Karanjkar M, Moholkar A, Gang M, Kim J and Patil P 2014 *Current Appl Phys* **14** 389
[27] Madhavi V, Kumar P J, Kondaiah P, Hussain O M and Uthanna S 2014 *Ionics* **20** 1737
[28] Lin Y S, Tsai T H, Lu W H and Shie B S 2014 *Ionics* **20** 116
[29] Gesheva K A 2007 *Thin Film Optical Coatings for Effective Solar Energy Utilization* Nova Science, NY, USA
[30] Gozde O I, Coclite A M and Gleason K K 2012 *Rep Prog Phys* **75** 016501
[31] Seidel S, Riche C and Gupta M 2011 *Chemical Vapor Deposition of Polymer Films. Encyclopedia Of Polymer Science and Technology*, John Wiley & Sons, Weinheim, Germany
[32] Drosos C and Vernardou D 2015 *Solar Energ Mater Solar Cell* **140** 1
[33] Pedersen H and Elliott S D 2014 *Theor Chem Acc* **133** 1476
[34] Gesheva K, Szekeres A and Ivanova T 2003 *Solar Energ Mater Solar Cell* **76** 563
[35] Ivanova T. Gesheva K, Kalitzova M, Marsen B, Cole B and Miller E L 2007 *Mater Sci Eng B* **142** 126
[36] Gesheva K A , Cziraki A,. Ivanova T and Szekeres A 2007 *Thin Solid Films* **515** 4609
[37] Gesheva K A, Ivanova T, Marsen B, Cole B, Miller E L and Hamelmann F 2007 *Surf Coat Technol* **201** 9378
[38] Liu Q, Dong G, Xiao Y, Gao F, Wang M, Wang Q, Wang S, Zuo H and Diao X 2015 *Mater Lett* **142** 232

[39] Wang Y J, Ouyang S H, Lu J G and Shieh H P D 2015 *SID DIGEST* 557
[40] Lee U J, Lee S-H, Yoon J, Oh S J, Lee S H and Lee J K 2013 *Solar Energ Mater Solar Cell* **108** 50
[41] Alzoubi K, Hamasha M M, Lu S, Sammakia B 2011 *J Display Technol* **7** 593
[42] Chou C S, Chou Ch Sh, Kuo Y T and Wang C P 2013 *Adv Powder Technol* **24** 336
[43] Cuong N K, Saeki N, Kataoka S and Yoshikawa S 2002 *Hyomen Kagaku* **23** 202
[44] Aleksandrova M, Kurtev N, Videkov V, Tzanova S and Schintke S 2015 *Microel Eng* **145** 112
[45] Wang G F, Tao X M, Xin J H and Fei B 2009 *Nanoscale Res Lett* **4** 613
[46] Aleksandrova M 2016 *Microel Intern* **33** in press
[47] Hoffmann M R, Martin S T, Choi W and Bahnemann D W 1995 *Chem Rev* **95** 69
[48] Hashimoto K, Irie H and Fujishima A 2006 *Jap J Appl Phys* **44** 8269
[49] Liu G, Wang L, Yang H G, Cheng H M and Lu G Q 2010 *J Mater Chem* **20** 831
[50] Czakkel O, Geissler E, Szilágyi I M and László K 2013 *Nanomater Env* **1** 23
[51] Szilágyi I M, Fórizs B, Rosseler O, Szegedi Á, Németh P, Király P, Tárkányi G, Vajna B, Varga–Josepovits K, László K, Tóth A L, Baranyai P and Leskelä M 2012 *J Catal* **294** 119
[52] George S M 2010 *Chem Rev* **110** 111
[53] Kim H, Lee H B R and Maeng W J 2009 *Thin Solid Films* **517** 2563
[54] Knez M, Nielsch K and Niinistö L 2007 *Adv Mater* **19** 3425
[55] Szilágyi I M, Nagy D 2014 *J Phys Conf Ser* **559** 012010
[56] Devi A 2013 *Coord Chem Rev* **257** 3332
[57] Bertuch A, Sundaram G, Saly M, Moser D and Kanjolia R 2014 *J Vac Sci Technol A* **32** 01A119
[58] Diskus M, Nilsen O and Fjellvåg H 2011 *J Mater Chem* **21** 705
[59] Mamun M, Zhang K, Baumgart H and Elmustafa A A 2015 J Solid State Sci Technol **4** P398
[60] Nandi D K and Sarkar S K 2014 *Energy Proc* **54** 782
[61] Malm J, Sajavaara T and Karppinen M 2012 *Chem Vapor Dep* **18** 245
[62] Dezelah IV C L, El-Kadri O M, Szilágy, I M, Campbel, J M, Arstila K, Niinistö L and Winter C H 2006 *J Am Chem Soc* **128** 9638
[63] Gesheva K A, Ivanova T, Marsen B, Zollo G, Kalitzova M 2008 *J Cryst Growth* **310** 2103
[64] Pore V, Ritala M, Leskelä M, Areva S, Järn M and Järnström J 2007 *J Mater Chem* **17** 1361
[65] Pore V, Kivelä T, Ritala M and Leskelä M 2008 *Dalton Trans* **45** 6467
[66] Szilágyi I M, Santala E, Heikkilä M, Kemell M, Nikitin T, Khriachtchev L, Räsänen M, Ritala M and Leskelä M 2011 *J Therm Anal Calorim* **105** 73
[67] Szilágyi I M, Santala E, Heikkilä M, Pore V, Kemel, M, Nikitin T, Khriachtchev L, Räsänen M, Ritala M and Leskelä M 2013 *Chem Vapor Dep* **19** 149
[68] Santala E, Kemell M, Leskela M and Ritala M 2009 *Nanotechnology* **20** 035602
[69] Kayaci F, Vempati S, Ozgit-Akgun C, Biyikli N and Uyar T 2014 *Appl Catal B* **156** 173
[70] Bao X Q and Liu L 2014 *J Power Source* **268** 677
[71] Szilágyi I M, Teucher G, Härkönen E, Färm E, Hatanpää T, Nikitin T, Khriachtchev L, Räsänen M, Ritala M and Leskelä M 2013 *Nanotechnology* **24** 245701